LincRNA-EPS increases TGF-β expression to inhibit the Wnt/β-catenin pathway, VSMC osteoblastic differentiation and vascular calcification in diabetic mice

YIBO LI[1*], ZIWEI XI[2*], ZHENG YU[3], CHAOYUE YANG[2] and CHUNHUA TAN[1]

[1]Department of Orthopedics, General Hospital of Central Theater Command (Hankou District), Wuhan, Hubei 430000;
[2]School of Medical Sciences, Army Medical University, Chongqing 400038;
[3]Department of Hematoendocrinology, 32295 Army Hospital, Liaoyang, Liaoning 111000, P.R. China

Abstract. In patients with diabetes, the Wnt/β-catenin pathway in vascular smooth muscle cells (VSMCs) is continuously activated by low-intensity inflammation, which leads to the osteoblastic differentiation of these cells and the deposition of calcium and phosphorus in blood vessels. The aim of the present study was to determine whether long intergenic non-coding RNA-erythroid pro-survival (lincRNA-EPS) was able to ameliorate vascular calcification (VC) associated with diabetes. VSMCs isolated from C57BL/6 mice were transfected with lincRNA-EPS overexpression vector *in vitro* and their osteoblastic differentiation was evaluated under high-glucose conditions. In addition, a mouse model of diabetes was established, which included a lincRNA-EPS knockout group and a lincRNA-EPS high expression group. Blood vessel samples from the mice were examined to determine the degree of calcification. The levels of inflammatory factors in serum were also detected. The VSMCs transfected with lincRNA-EPS overexpression vector exhibited less osteoblastic differentiation and migration and significantly lower levels of Wnt pathway-associated proteins than those transfected with empty control. Furthermore, the *in vivo* experiments revealed that the overexpression of lincRNA-EPS significantly reduced VC in diabetic mice. Therefore, on the basis of these findings, it is suggested that lincRNA-EPS overexpression may provide a novel and effective method for the treatment of VC in patients with diabetes.

Correspondence to: Dr Chunhua Tan, Department of Orthopedics, General Hospital of Central Theater Command (Hankou District), 68 Huangpu Avenue, Jiang'an, Wuhan, Hubei 430000, P.R. China
E-mail: tanchunhuadoc@163.com

*Contributed equally

Introduction

Diabetes mellitus is a chronic disease, which is becoming increasingly widespread globally. It causes several secondary complications, including heart disease, renal failure, blindness, nerve injury and vascular calcification (VC) (1,2). It has been reported that the global incidence of diabetes is 8.8%, and 70-80% of the affected population succumb to cardiovascular complications, making it the leading cause of mortality in patients with diabetes (3). VC is an important sign suggesting a high risk of cardiovascular disease (4). Although VC was previously considered to be a manifestation of the aging process, present research indicates that VC is a strictly regulated and active process, similar to bone formation (5). However, the mechanism of VC in a high-glucose (HG) environment is unclear. Macrophages have been shown to release numerous inflammatory cytokines, including tumor necrosis factor (TNF)-α, in a HG environment to maintain glucose and lipid homeostasis. These factors also maintain the body in a low-intensity inflammatory state, which can activate the Wnt/β-catenin pathway in vascular smooth muscle cells (VSMCs), leading to VC (6). In the process of VC, the osteoblastic differentiation of VSMCs is the most important step (5). Under normal conditions, VSMCs secrete a series of endogenous calcium inhibitors, including osteopontin, osteoprotegerin and matrix Gla protein, which inhibit osteoblastic differentiation (4). During VC, the levels of these endogenous calcium inhibitors are reduced by HG and low-intensity inflammation. In addition, the concentration of intracellular phosphate is increased by the sodium-dependent phosphate cotransporter Pit-1, which contributes to the transformation of VSMCs into osteoblast-like cells. Under the control of core binding factor A1, these osteoblasts express alkaline

phosphatase (ALP) and bone-related proteins such as osteo-calcin and bone morphogenetic protein-2, which further promote osteoblastic differentiation and the calcification of VSMCs (4). Hence, activation of the Wnt/β-catenin pathway in VSMCs under low-intensity inflammation may be a key cause of VC in HG conditions.

The Wnt/β-catenin pathway plays an important role in osteoblastic differentiation (7). Normally, without the intervention of Wnt proteins, a destruction complex is formed that is able to bind with and phosphorylate β-catenin in the cytoplasm and disable it. However, when Wnt protein is secreted, it combines with cell-surface receptors and helps the Axin component of the destruction complex to combine with phosphorylated low-density lipoprotein receptor-related protein, resulting in the breakdown of the destruction complex and the accumulation of high levels of β-catenin in the cytoplasm. β-catenin then enters the nucleus and binds with the DNA-binding T cell factor transcription factor, which activates Wnt gene transcription and recruits several transcriptional coactivators and histone modifiers, such as Brg1, CREB binding protein, Cdc47, Bcl9 and Pygopus, to drive target gene expression (8).

Transforming growth factor-β (TGF-β) is a multifunctional cytokine, which is highly expressed in most tumor cells and helps to regulate the Wnt/β-catenin pathway. In addition to promoting the epithelial-mesenchymal transition, invasion and metastasis of tumor cells, TGF-β serves an important role in the regulation of the adaptive immune system (9). TGF-β has been reported to inhibit the expression of various pro-inflammatory factors in macrophages, including interleukin (IL)-1β and IL-8, and to regulate TNF-α under certain conditions (10). Due to its anti-inflammatory effect, TGF-β may regulate the Wnt/β-catenin pathway, which is potentially the key cause of the phenotypic transformation of VSMCs and, therefore, is a potential therapeutic target.

Long intergenic RNA-erythroid pro-survival (lincRNA-EPS) activates TGF-β and thus inhibits the Wnt/β-catenin pathway (11). Therefore, lincRNA-EPS is indicated to be a regulatory factor that suppresses the dedifferentiation and transformation of VSMCs. lincRNAs are RNAs >200 nucleotides in length that control gene transcription by binding to chromatin-modifying factors, heteronuclear ribonucleoproteins or transcription factors (11). Although they lack protein-coding potential, they are important regulatory molecules for gene expression (12). lincRNA-EPS is expressed in macrophages and dendritic cells, where it inhibits macrophage function and the expression of inflammatory genes. A previous study demonstrated that lincRNA-EPS precisely regulates macrophages to inhibit the expression of inflammation-related genes (IRGs); a combination of gain-of-function and rescue experiments and the transcriptome analysis of mouse macrophages lacking lincRNA-EPS revealed the role of lincRNA as an inhibitor of IRG expression and repressor of inflammatory responses (11). Therefore, in the present study, the role of lincRNA-EPS in the process of VC was explored to determine its potential as a target for clinical treatment in the management of diabetic angiopathy.

In the present study, *in vivo* and *in vitro* models were used to study whether lincRNA-EPS affects the osteoblastic differentiation of mouse VSMCs. *In vitro*, VSMCs were transfected with lincRNA-EP empty control, lincRNA-EPS small interfering RNA (siRNA) or empty control and cultured in a HG environment. The ALP activity and expression of relevant proteins were observed using immunofluorescence and western blot analysis. An *in vivo* mouse model of diabetes was also established, and double lincRNA-EPS knockout and overexpression methods were used to study VC under various conditions.

Materials and methods

Animal experiments. A total of 20 six-week-old male C57BL/6 mice weighing 19-21 g, purchased from the Animal Center of Army Medical University were used for adaptive breeding for 1 week. Animal care and procedures were carried out with the approval of the Animal Management Committee of the General Hospital of Central Theater Command and strictly complied with the National Institutes of Health (NIH) Guide for the Care and Use of Laboratory Animals. The specific feeding environment was as follows: The temperature was controlled at 18-22˚C, with humidity at 50-60%. In order to keep the air fresh, the ammonia concentration did not exceed 20 ppm, and the ventilation times reached 10-20 air changes/h. The light intensity at 1 m from the ground was 200 lux, and the light/dark cycle was 12:12. Food from Jiangsu Xietong Pharmaceutical Bio-engineering Co., Ltd. was eaten at 3-7 g/day, supplied 3-4 times per week. Water was supplied through drinking bottles. Of these, 10 randomly selected mice were given normal feed and the other 10 mice were given high-fat feed (40% fat, 42% carbohydrate and 18% protein). After 1 month of feeding and fasting for 12 h (overnight), the mice fed a high-fat diet were injected intraperitoneally with 100 mg/kg streptozotocin (dissolved in 0.1 mol/l sodium citrate buffer; pH 4.2), while the mice fed a normal diet were given a similar volume of sodium citrate buffer. After 7 days, blood glucose levels were checked and the mice with fasting blood glucose levels ≥11.1 mmol/l were considered as a suitable model for diabetes (13,14). A wild-type group was created by the random selection of six mice from those that met the criteria for the diabetic model. A total of 6 mice were randomly selected from the 10 mice given normal feed to form the control group.

Chemicals. Parathyroid hormone (PTH; cat. no. H207) and ALP (cat. no. A059-2-2) ELISA kits were purchased from Nanjing Jiancheng Bioengineering Institute. The fibroblast growth factor-23 (FGF-23) ELISA kit (cat. no. EM0271) was purchased from Wuhan Fine Biotech Co., Ltd. Fetal bovine serum (FBS; cat. no. 30067334) was purchased from Gibco (Thermo Fisher Scientific, Inc.). DMEM (cat. no. SH30021.01), streptomycin (cat. no. SV30010) and penicillin (cat. no. SV30010) were purchased from HyClone (Cytiva). TRIzol® reagent (cat. no. 15596018) was purchased from Invitrogen (Thermo Fisher Scientific, Inc.). The BCA kit (cat. no. C503021-0500) was purchased from Sangon Biotech Co., Ltd.

VSMC culture. After feeding, 12 male C57BL/6 mice (6-week-old, weighing 19-21 g) from two groups were euthanized with CO_2. The flow rate of CO_2 was 10-30% of the euthanasia chamber volume/min, and the mice were exposed to 100% CO_2 for 5 min. After their vital signs disappeared,

the mice were observed for 2 min to confirm their death. The common carotid artery was then surgically removed. The adventitia of the aorta was removed and cut into 1-mm^2 tissue blocks, which were cultured in primary culture medium for 3-5 generations to provide VSMCs. The VSMC culture medium comprised α-MEM (cat. no. SH30265.01; HyClone; Cytiva) supplemented with 10% FBS, 100 U/ml penicillin and 0.1 mg/ml streptomycin.

LincRNA-EPS fragment transfection into VSMCs. The cultured VSMCs were used to establish normal, empty control (empty vector), lincRNA-EPS overexpression vector, lincRNA-EPS siRNA and si-negative control (NC) groups. The VSMCs were digested with 0.125% trypsin for ~2 min. After centrifugation at 100 x g at 25°C for 10 min, the VSMCs were seeded at a density of 1x10^4 cells/cm^3 into 6-well plates and cultured for 24 h. When the cells had grown to 60-70% confluence, the medium was changed to a serum-free medium. The VSMCs were then transfected with 200 nM si-negative control (NC) or lincRNA-EPS siRNA, or with 2.5 μg plasmid containing lincRNA-EPS overexpression or empty control (Thermo Fisher Scientific, Inc.), using the Lipofectamine® 2000 transfection kit (cat. no. 11668027; Thermo Fisher Scientific, Inc.). After 6 h, transfection was terminated, and culture was continued for 24 h. Reverse transcription-quantitative PCR (RT-qPCR) was used to detect the expression of lincRNA-EPS in the RNA extracts from the cells collected from each group.

The lincRNA-EPS overexpression sequence was synthesized according to the full-length cDNA of mouse lincRNA-EPS, and the sequence was synthesized according to its coding sequence (Sangon Biotech Co., Ltd.). The VSMCs in the empty control group were transfected with scrambled controls (Thermo Fisher Scientific, Inc.) that were cloned into an expression vector; specifically, the complete mouse lincRNA-EPS and scrambled sequences (Appendix S1) were subcloned into the adenoviral shuttle vector pDC315 (Microbix Biosystems Inc.). The siRNA sequences used were as follows: si-EPS1 forward, 5'-GGU UUAGCACUCACUGCUAGC-3' and reverse, 5'-UAGCAG UGAGUGCUAAACCGU-3'; si-EPS2 forward, 5'-CGC AUGGUCACUCACCUAAUA-3' and reverse, 5'-UUAGGU GAGUGACCAUGCGUG-3'; si-EPS3 forward, 5'-CAUGGU CACUCACCUAAUAAG-3' and reverse, 5'-UAUUAGGUG AGUGACCAUGCG-3'. si-NC sequences were as follows: si-NC forward, 5'-UUCUCCGAACGUGUCACGUTT-3' and reverse, 5'-ACGUGACACGUUCGGAGAATT-3' was purchased from General Biosystems (Anhui) Co., Ltd. All siRNA groups were tested and si-EPS1 was selected in the end.

LincRNA-EPS knockout mice. Under the control of a phosphoglycerate kinase 1 promoter, the 4-kb lincRNA-EPS genomic site was replaced with a neomycin cassette to generate lincRNA-EPS knockout mice as previously described (11). In brief, a lincRNA-EPS targeting vector was electroporated into C57BL/6 mice embryonic stem (ES) cells and the lincRNA-EPS-positive ES cells were injected into blastocyst-stage embryos to produce chimeric mice. lincRNA-EPS heterozygous mice were obtained by gamete line transmission after mating the chimeric mice with wild-type C57BL/6

mice The resulting gene knockout mice were designated the lincRNA-EPS knockout group (lincRNA-EPS$^{-/-}$). The lincRNA-EPS knockout group contained 6 male mice, which were supplied with a high-fat diet.

Overexpression of lincRNA-EPS in mice. Using a WAVE Bioreactor system (GE WAVE 200; Cytiva), an adeno-associated virus (AAV) with high expression of lincRNA-EPS was constructed, packaged in 293 cells (cat. no. CL-0005; Procell Life Science & Technology Co., Ltd.) and purified as required. In six-well dishes, 1.2x10^6 subconfluent 293 cells (15) were transfected with 2.5 μg plasmid (pAAV-CMV-EGFP-P2A-lincRNA-EPS-3FLAG; designed by OBiO Technology (Shanghai) Corp., Ltd.) at 4°C for 20 min. A total of six 6-week-old male C57BL/6 mice weighing 19-21 g were injected with 1x10^{11} AAV particles via the tail vein (16). These mice were designated as the lincRNA-EPS overexpression group (lincRNA-EPS$^{Tg/+}$). The 6 mice in the lincRNA-EPS overexpression group were supplied with a high-fat diet. After 6 weeks, the mice from the lincRNA-EPS knockout and overexpression groups were euthanized with CO$_2$, and 5 ml of blood were sampled for the extraction of macrophages and T cells. The expression of lincRNA-EPS in these cells was detected using RT-qPCR to confirm the success of the transfection models (17-19).

Harvesting, cell lysis and clarification. The mice were euthanized and their spleen was removed under sterile conditions. The spleen was ground on a filter screen using the piston of the syringe for 5 min. The grinding product was put in 4-5 ml Mouse Lymphocyte Separation Medium (cat. no. 7211011; Dakewe Biotechnology Co., Ltd.), 500 μl RPMI-1640 medium were added. Subsequently, the samples were centrifuged at 800 x g at 25°C for 30 min. The upper cell suspension was added to 10 ml of RPMI-1640 medium, and centrifuged at 250 x g at 25°C for 10 min. After the supernatant was removed, lympho Spot™ medium (Dakewe Biotechnology Co., Ltd.) was added to the sediment, and the T cells were counted.

In order to extract macrophages, a total of 1 ml starch broth was injected into the abdominal cavity of mice for 3 days, then DMEM medium was injected, fully mixed, sucked out, centrifuged and resuspended.

RT-qPCR. The VSMCs, macrophages and T cells were lysed using TRIzol® reagent according to the manufacturer's instructions. RNA was extracted with isopropanol after centrifuging the lysate with chloroform at 1,200 x g at 4°C for 10 min. The pellet was washed and resuspended in 75% ethanol, then air-dried for 10 min. Then, 20 μl TE buffer at 60°C was added. After incubating for 10 min, the quality of the RNA was checked, and those samples that passed the quality test were stored at -70°C.

The following primers were designed: ALP forward, 5'-GCCGCACCACGACTTGTTCA-3' and reverse, 5'-GCG ATCGTGTTGGCGAGAAC-3' (150 bp); Wnt3 forward, 5'-AGCTGCCTCTACTCGTGACA-3' and reverse, 5'-ATC TTGCTCCCACTGTTGGC-3' (194 bp). TGF-β1 forward, 5'-TGGAGCAACATGTGGAACTC-3' and reverse, 5'-GTC AGCAGCCGGTTACCA-3' (73 bp). β-catenin forward, 5'-ACAGGGAAGACATCACTGAGCC-3' and reverse,

5'-CAG TGG GAT GGT GGG TGT AAG A-3' (145 bp); lincRNA-EPS forward, 5'-CGCATTAATGGGGGCATTC-3' and reverse, 5'-CTAAACCGTGTTTTCCCCGC-3'; GAPDH forward, 5'-GAAGGGTGGAGGCAAAAG-3' and reverse, 5'-ACCAGTGGTTGCAGGGAT-3'. The reverse transcription kit (cat. no. 11939823001; the Licensing Department of Roche Molecular Diagnostics, Inc.) was used to synthesize cDNA from the RNA according to the manufacturer's protocol. The RT-qPCR system was configured for each group of cDNA samples accordingly. qPCR was conducted using a SYBR premix Ex Taq™ kit (Takara Bio, Inc.) according to the manufacturer's instructions. A total of 40 PCR cycles (94°C for 1 min for denaturation; 55°C for 30 sec for annealing; 72°C for 1 min for extension) were performed and melting curves of the PCR products were established to determine the expression of ALP, Wnt3, β-catenin and TGF-β (20).

HG culture and ALP ELISA. According to a previously reported method (21), common carotid artery samples were taken from 6-week-old mice and the transfected VSMCs were cultured under HG conditions (25 mM) while the untransfected VSMCs were cultured under normal glucose conditions. The temperature was 25°C and the culturing time was 3 days. Subsequently, the ALP-ELISA kit was used to determine the ALP levels of the samples.

Western blot analysis. The total proteins were extracted from VSMCs using RIPA lysis buffer (cat. no. 2114-100; BioVision, Inc.). The proteins were then quantified using a BCA kit, denatured at 100°C for 10 min and stored at -80°C. Western blotting was used to determine the expression levels of ALP, TGF-β, Wnt3 and β-catenin. A total of 100 μg of protein per sample was loaded on a 10% SDS-PAGE gel. The proteins were subsequently transferred to PVDF membranes, then blocked with 5% non-fat milk powder at 25°C for 60 min. The membranes were washed with PBS buffer containing 0.1% Tween. GAPDH antibody (cat. no. 51332S; Cell Signaling Technology, Inc.), ALP antibody (cat. no. ab67228; Abcam), TGF-β antibody (cat. no. 3711S; Cell Signaling Technology, Inc.), Wnt3 antibody (cat. no. ab32249; Abcam) and β-catenin antibody (cat. no. AC106; Beyotime Institute of Biotechnology) were used at 1:1,000 dilution at 25°C for 2.5 h. The membranes were subsequently incubated with HRP-labeled Goat Anti-Mouse IgG (H+L) secondary antibodies (cat. no. A0216; Beyotime Institute of Biotechnology) diluted by 1:1,000 at 25°C for 1 h. Antibody detection was performed with an ECL kit from Shanghai Zeye Biotechnology Co., Ltd. (cat. no. ZY120201).

Luciferase reporter assay. VSMCs were cultured in 24-well plates and co-transfected with luciferase reporter plasmids and lincRNA-EPS overexpression vector, inhibitor or their respective controls and 50 ng per well of pRL-TK vector (designed by Promega Corporation) using Lipofectamine® 2000 (Invitrogen; Thermo Fisher Scientific, Inc.) at 25°C for 20 min according to the manufacturer's instructions. After co-transfection, VSMCs were collected 48 h later and lysed prior to the measurement of luciferase activity with the Dual-Luciferase Reporter Assay System (Promega Corporation). *Renilla* luciferase activity was used for normalization (22).

Alizarin red S staining. To evaluate the inhibitory effect of lincRNA-EPS on VC *in vitro*, VSMCs transfected with 200 nM empty control, lincRNA-EPS overexpression or lincRNA-EPS siRNA using Lipofectamine® 2000 were cultured in DMEM for 7 days. After washing, the cells were fixed in 4% formalin at 25°C for 24 h, then stained with 1% alizarin red S at 37°C for 30 min. The VSMCs were washed with PBS to remove the excess stain and photographic images of the stained matrix were captured using a digital microscope. The VSMCs were then incubated in cetyl-pyridinium chloride for 15 min to release the alizarin red S, and the amount of released dye was measured by spectrophotometry at 570 nm.

Scratch wound assay. A total of $1x10^6$ cells/ml VSMCs (23) were seeded onto 12-well culture plates and cultured overnight, after which mitomycin (5 μg/ml, Bio-Rad Laboratories, Inc.) was added for 2 h. Then, a sterile P-200 pipette tip was used to create an artificial wound in each well. After 12 h of culture in the presence of 1% FBS, the cells were stained with crystal violet at 25°C for 10 min and evaluated using light microscopy (cat. no. DVM6; Leica Microsystems GmbH). The results were analyzed using ImageJ software v. 1.8.0.112 (National Institutes of Health).

Morphological and immunofluorescence analysis. Aortic tissue was fixed at 4°C overnight in 4% formalin and embedded in paraffin. The tissues were cut into 40-μm-thick sections. For immunofluorescence analysis, the sections were first immersed in boiling citric acid buffer (95°C) for 10 min to restore antigenicity and then soaked in 0.3% H_2O_2 at 95°C for 30 min to eliminate endogenous peroxidase. Subsequently, the sections were blocked with 5% goat serum (cat no. KJ-S-0028G; Kejing Biological Technology Co., Ltd.) at 25°C for 30 min. Next, after washing with PBS, the sections were incubated with Runt-related transcription factor 2 (Runx2; 1;1,000; cat. no. ab76956; Abcam) for 2 h at 25°C. After washing, the sections were incubated with fluorescent secondary antibodies (1:1,000; cat. no. AB_2534088; Thermo Fisher Scientific, Inc.) for 1 h at 25°C, then counterstained with DAPI for 10 min at 25°C. Finally, the sections were stained with diaminobenzidine and visualized using a light microscope (24).

Cytokine analysis. For the detection of cytokines, 0.2 ml of blood was collected from each mouse under anesthesia (1-1.5% isoflurane; Abbott Scandinavia AB) by retroorbital vein puncture. This procedure was only performed once after 6 weeks of feeding. After the blood was collected, rearing of the mice continued until they were required for further analysis. ELISA kits were used to detect the expression of inflammation-associated factors in the serum of each group, including IL-1β (cat. no. E-EL-M0037c; Elabscience Biotechnology, Inc.), TNF-α (cat. no. PT512; Beyotime Institute of Biotechnology), IL-6 (cat. no. E-EL-M0044c; Elabscience Biotechnology Co., Ltd.) and nitric oxide (NO; cat. no. YM-6178; Shanghai Yuanmu Biological Technology Co., Ltd.).

Biochemical analysis. The mice were euthanized with CO_2, and 5 ml blood and the aortas were retrieved. The aortas of the experimental mice were rinsed with distilled water, dried and weighed. The weight of every group was controlled to
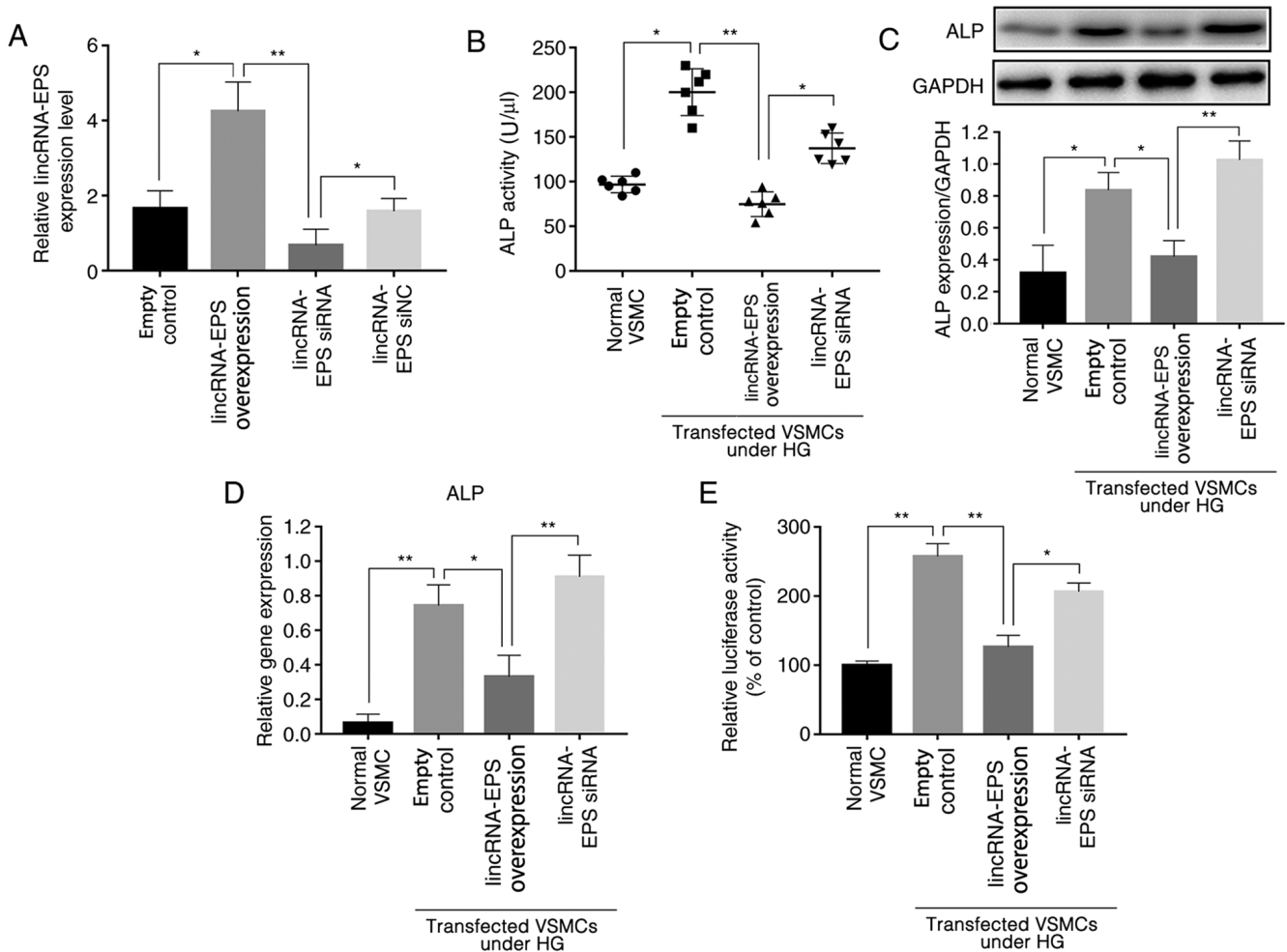
Figure 1. lincRNA-EPS suppresses the osteoblastic differentiation of VSMCs. (A) RT-qPCR results show the transfection efficiency of lincRNA-EPS over-expression vector and siRNA. (B) ALP activity of aortic VSMCs detected using ELISA. (C) ALP activity of aortic VSMCs detected by western blot analysis. (D) RT-qPCR results show the mRNA levels of ALP in aortic VSMCs. (E) ALP promoter activity detected by a relative luciferase assay. n=6 independent experiments. *P<0.05 and **P<0.01 as indicated. lincRNA-EPS, long intergenic non-coding RNA-erythroid pro-survival; siRNA, small interfering RNA; siNC, small interfering negative control; VSMCs, vascular smooth muscle cells; ALP, alkaline phosphatase; HG, high glucose.

3 mg. The blood was collected into anticoagulation tubes (BD Biosciences). After 3,000 x g centrifugation for 30 min at 4˚C, the supernatant of blood was taken as plasma. ELISA kits were used to quantify FGF-23 and PTH levels in plasma according to the manufacturer's instructions.

Calcium deposition. The quantification of aortic calcium was carried out by incubating the tissues at 37˚C overnight in 0.6 M HCl. The calcium content of the supernatant was then determined using a QuantiChrom™ Calcium assay kit (BioAssay Systems) according to the manufacturer's protocol. The total protein concentration was measured using the Bradford method (Bio-Rad Laboratories, Inc.). The VSMCs were decalcified for 24 h at 4˚C in 0.6 M HCl. The calcium content was then determined using the aforementioned QuantiChrom™ Calcium assay kit. The VSMCs were lysed with 0.1 M NaOH/0.1% SDS. The calcium content was normalized to the total protein concentration.

Statistical analysis. For multiple group comparisons, one-way ANOVA with Tukey's post hoc test were performed. P<0.05 was considered to indicate a statistically significant difference.

GraphPad Prism 7 (GraphPad Software, Inc.) was used for graph construction and statistical analyses (20).

Results

LincRNA-EPS transfection inhibits HG-induced osteoblastic differentiation in mouse VSMCs by reducing ALP levels. Previous studies have shown that ALP activity is an indicator of the osteoblastic differentiation of VSMCs (25,26) and that ALP is a significant factor in the regulation of this process; higher ALP levels are associated with higher osteoblastic differentiation (25,26). Experiments were performed using mouse VSMCs transfected with lincRNA-EPS overexpression vector or siRNA, and RT-qPCR analysis verified the transfection efficiency (Fig. 1A). The ALP activity of various wild-type mouse VSMCs was tested using an ALP ELISA kit, and the results showed that, under HG conditions, the ALP activity of VSMCs transfected with lincRNA-EPS overexpression vector was reduced by an average of 62.5% compared with that of cells transfected with the empty control, and of 35% in the lincRNA-EPS siRNA group (Fig. 1B). For further analysis, western blotting was used to detect the expression levels of

ALP protein, and the results showed that expression of ALP in VSMCs after transfection with lincRNA-EPS overexpression vector was reduced by an average of 50% compared with that of cells transfected with the empty control while, contrarily, an increase by 25% was observed in the lincRNA-EPS siRNA group (Fig. 1C). The expression of ALP mRNA was also detected using RT-qPCR (Fig. 1D), and the results revealed that the average expression of ALP was reduced by 57% by the lincRNA-EPS overexpression vector, and by 20% by the lincRNA-EPS siRNA compared with the empty control. In addition, the luciferase reporter assay showed that the ALP gene promoter activity in wild-type VSMCs transfected with lincRNA-EPS overexpression vector was downregulated by 50% compared with that in the empty control group, while ALP gene expression in VSMCs transfected with lincRNA-EPS overexpression vector was downregulated by 50% compared to that in the control group and no obvious downregulation was observed in the lincRNA-EPS siRNA group (Fig. 1E). The present findings suggest that the transfection of lincRNA-EPS has a significant inhibitory effect on the expression of ALP, indicating that it may affect the osteoblastic differentiation of VSMCs.

LincRNA-EPS transfection inhibits HG-induced VSMC migration and calcification. HG triggers calcium deposition in wild-type VSMCs, which may result from the osteoblastic differentiation of VSMCs (27,28). Alizarin red S staining revealed that, in HG conditions, calcium deposition was significantly inhibited in VSMCs following transfection with lincRNA-EPS overexpression vector compared with empty control. However, calcium deposition remained at higher levels in the VSMCs transfected with the lincRNA-EPS siRNA (Fig. 2A). The absorbance of Alizarin red from the VSMCs in each group was measured using spectrophotometry to evaluate the osteogenic differentiation of VSMCs in each group. The absorbance value of the empty control group was set at 1.0 and the relative absorbance value of the lincRNA-EPS over-expression transfection group was 0.35. The absorbance of the VSMCs transfected with lincRNA-EPS overexpression vector was lower than those transfected with empty control and the lincRNA-EPS siRNA group (Fig. 2A). In the wound healing assay, microscopy was used to observe the migra-tion of VSMCs in each group. HG increased the migration of VSMCs by 175% compared with that of VSMCs under normal conditions. However, migration was reduced by 50% following transfection with lincRNA-EPS overexpression vector compared with the empty control (Fig. 2B).

LincRNA-EPS activates TGF-β to suppress inflammation and inhibits HG-induced Wnt pathway activation. Results from western blot analysis showed that, under HG conditions, Wnt3 expression decreased by 50%, β-catenin expression decreased by 46% and TGF-β expression increased by 70% in the lincRNA-EPS overexpression group compared with the empty control group, indicating that lincRNA-EPS significantly inhibited the expression of Wnt3 and β-catenin proteins and increased that of TGF-β (Fig. 3A and B). RT-qPCR results showed that, in the lincRNA-EPS overexpression group, Wnt3 levels were reduced by 36%, β-catenin levels were reduced by 50% and TGF-β levels were increased by 128% compared with
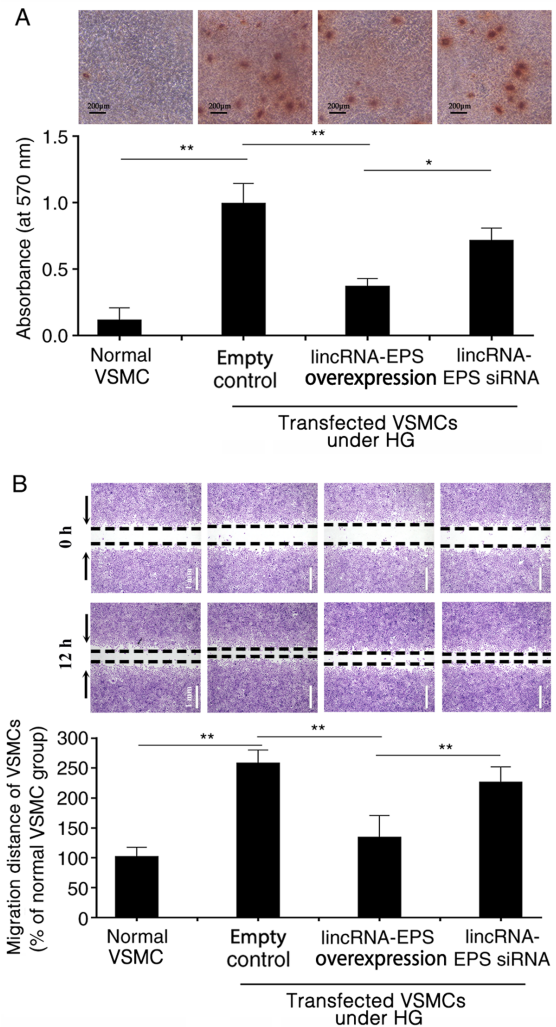

Figure 2. Effect of lincRNA-EPS on the osteoblastic differentiation and migration of VSMCs. (A) Osteoblastic differentiation detected in VSMCs using alizarin red S staining. Scale bar=200 μm. (B) Effects of different transfections on VSMC migration in a scratch healing assay. The migration distance of VSMCs at 12 h was analyzed. Scale bar=1 mm. n=6 independent experiments. *P<0.05 and **P<0.01 as indicated. lincRNA-EPS, long inter-genic non-coding RNA-erythroid pro-survival; siRNA, small interfering RNA; VSMCs, vascular smooth muscle cells; HG, high glucose.

those in the empty control group, suggesting that lincRNA-EPS significantly inhibited Wnt3 and β-catenin protein expression and enhanced TGF-β expression due to the upregulation of the mRNA expression of TGF-β and downregulation of the mRNA expression of Wnt3 and β-catenin in VSMCs (Fig. 3C). Immunofluorescence staining (Fig. 3D) further demonstrated that transfection with lincRNA-EPS overexpression vector reduced the expression of β-catenin.

LincRNA-EPS reduces the levels of inflammatory factors in the plasma of diabetic mice. After knocking out lincRNA-EPS from mice, there was a significant increase in the levels of several inflammatory factors, including NO, IL-1β, IL-6 and TNF-α. Among them, NO increased by 100% (Fig. 4A), IL-1β by 56% (Fig. 4B), IL-6 by 60% (Fig. 4C) and TNF-α by 28% (Fig. 4D) compared with those in wild-type mice. In the mice with lincRNA-EPS overexpression, the levels of these inflammatory factors were noticeably reduced
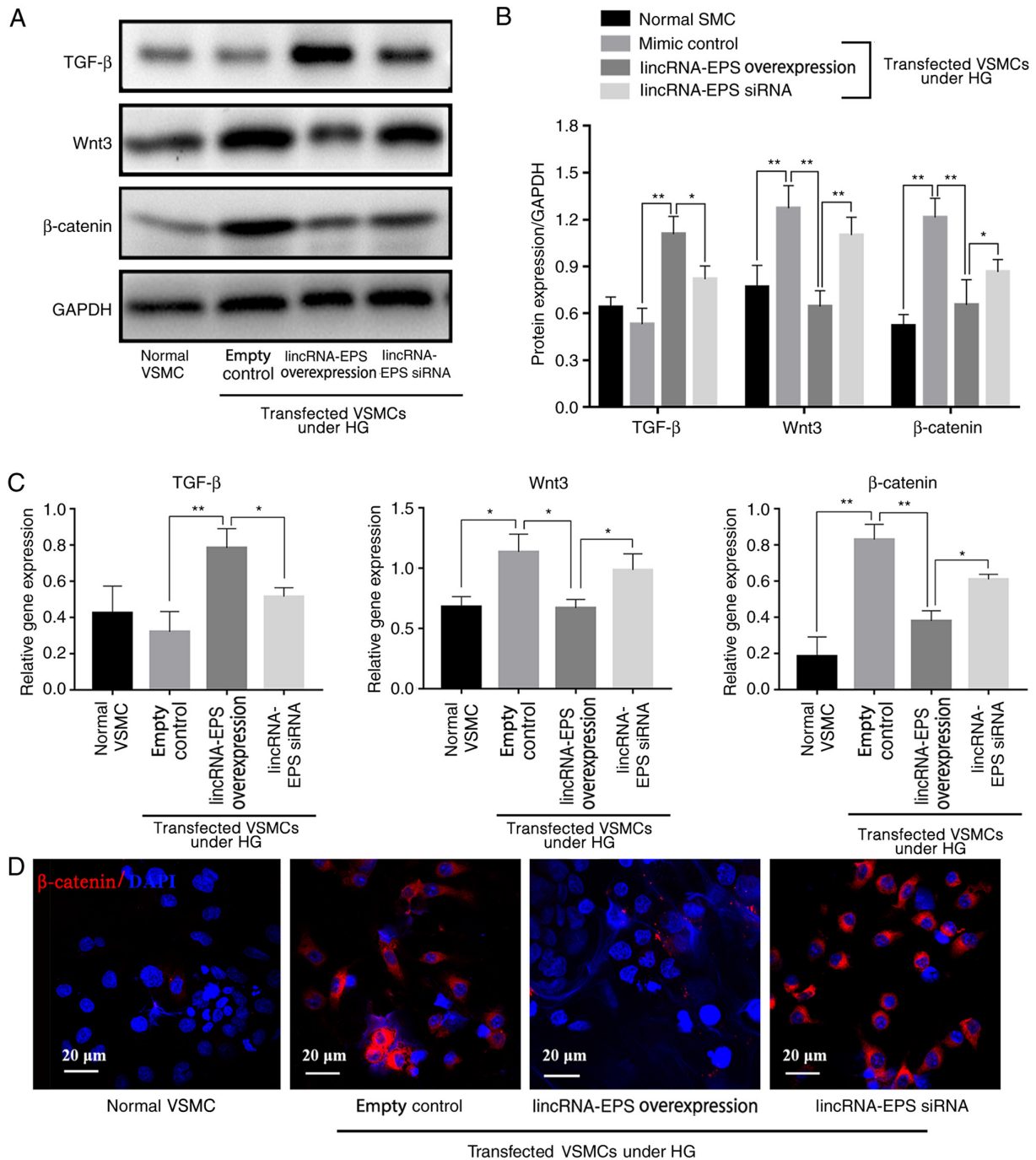
Figure 3. lincRNA-EPS affects the expression of TGF-β, Wnt3, and β-catenin in VSMCs. (A) Cellular protein levels of TGF-β, Wnt3 and β-catenin determined by western blotting. (B) Quantification of the protein levels of TGF-β, Wnt3 and β-catenin from the western blots. (C) mRNA levels of TGF-β, Wnt3 and β-catenin. (D) Immunofluorescence staining of β-catenin with DAPI nuclear counterstaining. Scale bar=20 μm. n=6 independent experiments. *$P<0.05$ and **$P<0.01$ as indicated. lincRNA-EPS, long intergenic non-coding RNA-erythroid pro-survival; siRNA, small interfering RNA; VSMCs, vascular smooth muscle cells; HG, high glucose.

compared with those of the wild-type control. The present results indicated the significance of lincRNA-EPS in the suppression of inflammation.

LincRNA-EPS inhibits VC in the diabetic mouse model. Runx2 is a transcription factor that can induce Sp7, another important transcription factor, which is able to promote the osteoblastic differentiation of VSMCs through the Wnt pathway (28). As shown in Fig. 5A, Runx2 expression was low in the aorta of the control group and abundant in the lincRNA-EPS$^{-/-}$ group,

but notably reduced in the lincRNA-EPS$^{Tg/+}$ group compared with that in the wild-type diabetic group. These results suggest that lincRNA-EPS may affect the osteoblastic differentiation of VSMCs by suppressing the expression of Runx2. As illustrated in Fig. 5B-E, compared with the wild-type diabetic group, the levels of vascular calcium, vascular phosphate and serum PTH in the lincRNA-EPS$^{Tg/+}$ group were notably reduced and the levels of serum FGF-23, a blood phosphorus-regulating hormone that promotes the excretion of phosphate, were increased. Specifically, vascular calcium
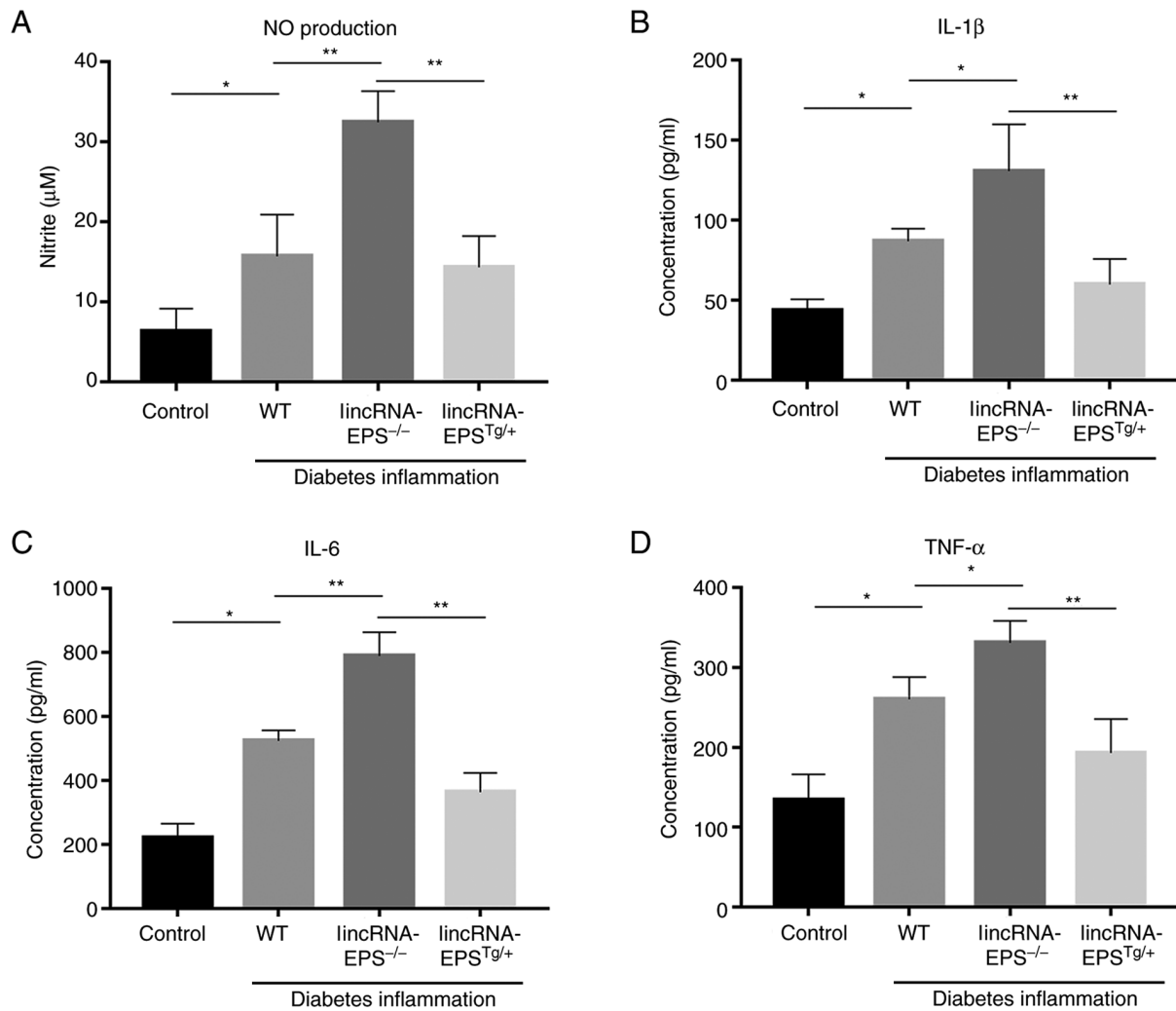
Figure 4. ELISAs were used to measure the levels of inflammatory factors in the serum of C57BL/6 mice. Levels of (A) NO production, (B) IL-1β, (C) IL-6 and (D) TNF-α. n=6 independent experiments. *P<0.05 and **P<0.01 as indicated. NO, nitric oxide; IL, interleukin; TNF-α, tumor necrosis factor-α; WT, wild type; lincRNA-EPS, long intergenic non-coding RNA-erythroid pro-survival; lincRNA-EPS^{-/-}, lincRNA-EPS knockout; lincRNA-EPS[Tg/+], lincRNA-EPS overexpression.

decreased by 50%, vascular phosphate by 18% and serum PTH by 7%, while serum FGF-23 increased by 25%. The present results confirmed the positive impact of lincRNA-EPS on VC in diabetic mice. Finally, the relative lincRNA-EPS expression levels of macrophages and T cells in the lincRNA-EPS^{-/-} and lincRNA-EPS[Tg/+] groups were measured and compared with those in the wild-type group to confirm that the mouse models had been successfully established (Fig. 6).

Discussion

VC is a key risk index of cardiovascular disease and a common cause of mortality in patients with diabetes. However, the drugs currently used to treat VC in patients with diabetes lack efficacy, which is problematic for patients and doctors.

Previous studies have provided evidence to show that the osteoblastic differentiation of VSMCs is an important mechanism for the development of VC (29-31). In the present study, the results of western blot analysis revealed the low expression of TGF-β and high expression of Wnt3 and β-catenin in empty control-transfected VSMCs under HG conditions. However,

in the HG environment, transfection with lincRNA-EPS increased the expression of TGF-β and decreased the expression of Wnt3 and β-catenin. In addition, a series of experiments demonstrated that ALP decreased significantly in VSMCs transfected with lincRNA-EPS overexpression vector and increased in those transfected with lincRNA-EPS siRNA. In addition, using Alizarin red S staining, it was shown that lincRNA-EPS-transfected VSMCs had less calcium deposition than the empty control-transfected VSMCs when cultured in a HG environment. Furthermore, the cell-migration distance of the lincRNA-EPS-transfected VSMCs was smaller than that of the empty control VSMCs. Based on the results of the present experiments, it may be inferred that TGF-β played a role in VC. Additionally, when levels of TGF-β are higher osteoblasts are less likely to differentiate. This is because high levels of TGF-β interfere with the Wnt/β-catenin pathway in VSMCs activated by continuous inflammation, which is responsible for the osteoblastic differentiation of VSMCs (22). However, the results of the present study indicated that the high expression of lincRNA-EPS regulated the Wnt/β-catenin pathway and affected the osteoblastic differentiation of VSMCs by
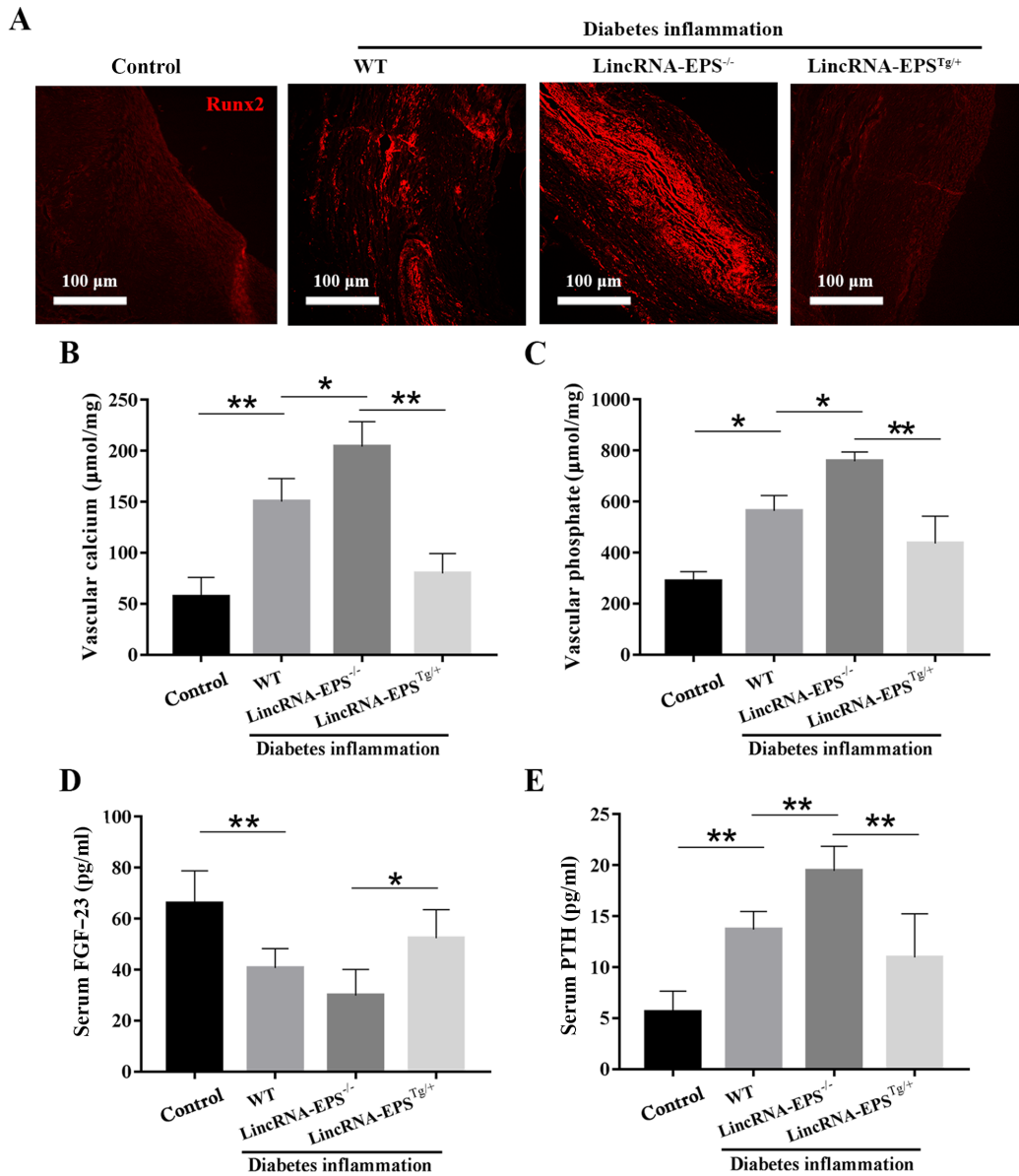
Figure 5. Effects of lincRNA-EPS on vascular calcification in diabetic C57BL/6 mice. (A) Aortic immunofluorescence staining showing the level of Runx2. Scale bar=100 μm (B) Aortic calcium level, (C) aortic phosphate level, (D) serum FGF-23 level and (E) serum PTH level. n=6 independent experiments. *P<0.05 and **P<0.01 as indicated. WT, wild type; lincRNA-EPS, long intergenic non-coding RNA-erythroid pro-survival; lincRNA-EPS^{-/-}, lincRNA-EPS knockout; lincRNA-EPS[Tg/+], lincRNA-EPS overexpression; Runx2, Runt-related transcription factor 2; FGF-23, fibroblast growth factor-23; PTH, parathyroid hormone.
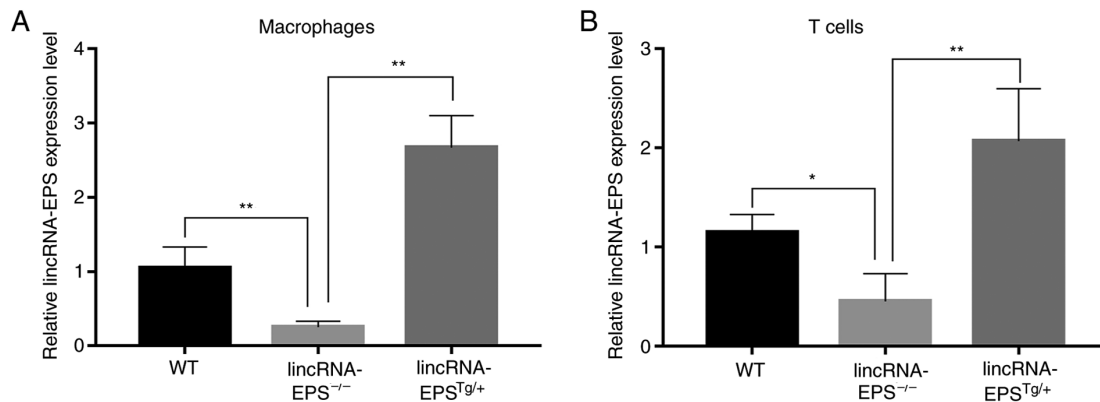

Figure 6. Relative lincRNA-EPS expression levels shows that the animal models were successfully established. Relative lincRNA-EPS expression level of (A) macrophages and (B) T cells. n=6 independent experiments. *P<0.05 and **P<0.01 as indicated. lincRNA-EPS, long intergenic non-coding RNA-erythroid pro-survival; lincRNA-EPS^{-/-}, lincRNA-EPS knockout; lincRNA-EPS[Tg/+], lincRNA-EPS overexpression.

promoting the expression of TGF-β and reducing Wnt3 and β-catenin expression.

In the present study, the overexpression of lincRNA-EPS in VSMCs was indicated to inhibit the osteoblastic differentiation of VSMCs and reduce the deposition of calcium and phosphate, thus significantly reducing the degree of VC. As mentioned above, the present study revealed that, with an increase in TGF-β levels, both Wnt3 and β-catenin were downregulated in VSMCs overexpressing lincRNA-EPS. In addition, significantly increased levels of IL-1β, IL-6 and TNF-α were detected in the plasma of lincRNA-EPS knockout diabetic mice. A previous study has demonstrated that TGF-β downregulated several pro-inflammatory factors in cells, including VSMCs, in atherosclerosis (32). In addition, TGF-β can promote the transformation of VSMCs from a quiescent, contractile state to an active state in which they can repair themselves (32). Several inflammatory factors promote the upregulation of inducible nitric oxide synthase expression in inflammatory cells (33) to produce large quantities of NO, as observed in the lincRNA-EPS knockout diabetic mice. NO can react with superoxide anions to form peroxynitrite (33) and can also increase the permeability of the microvasculature to promote the exudation of cells and serum via IL-2, both of which may cause sustained low-level inflammation (34,35). In the present study, serum analysis revealed significantly decreased FGF-23 levels and significantly increased PTH levels in lincRNA-EPS knockout diabetic mice, which are indicative of a significant disorder of calcium and phosphorus metabolism in the mice. Therefore, it may be concluded that the persistent low-level inflammation in the lincRNA-EPS knockout diabetic mice was associated with a disorder of calcium and phosphorus metabolism. FGF-23 promotes phosphate excretion by reducing the reabsorption of renal phosphate and reducing the level of PTH, a hormone that can induce VC, by reducing parathyroid secretion (36,37). When blood vessel samples from the mice were analyzed using Runx2 immunostaining, the results indicated that the degree of VC in the lincRNA-EPS knockout diabetic mice was higher than that in wild-type diabetic mice, while that in the lincRNA-EPS overexpressing diabetic mice was lower. These results collectively suggest that the high expression of lincRNA-EPS ameliorates VC; therefore, it may have a bright future in the management of diabetes. However, any adverse effects of the high expression of lincRNA-EPS require further exploration.

In conclusion, the present study demonstrated the effect of the overexpression of lincRNA-EPS in diabetes-induced VC. lincRNA-EPS was shown to regulate the Wnt/β-catenin pathway by promoting the expression of TGF-β and interfering with the expression of Wnt3 and β-catenin, thereby inhibiting the osteoblastic differentiation of VSMCs. These findings may potentially help to reduce or prevent VC in patients with diabetes and lower the risk of cardiovascular disease. In the future, lincRNA-EPS overexpression may be used as a novel treatment approach or preventive drug to delay the development of VC in patients with diabetes.

The timely resolution of inflammation in patients with diabetes is necessary to reduce the activation of the Wnt/β-catenin pathway resulting from the disordered calcium and phosphorus metabolism caused by inflammation. This may prevent the osteoblastic differentiation of VSMCs and the deposition of calcium and phosphorus in blood vessels. In addition, the present study suggested that lincRNA-EPS inhibits the expression of various inflammatory factors by increasing TGF-β levels and can inhibit the Wnt/β-catenin pathway to reduce inflammation, thereby potentially helping to prevent VC. In patients with diabetes, inflammation is generally the key cause of VC. Therefore, this study may serve as an innovative and useful starting point for the treatment of VC in patients with diabetes.

Availability of data and materials

The datasets used and/or analyzed during the current study are available from the corresponding author on reasonable request.

Authors' contributions

CT, YL and ZY conceptualized the study. ZX, CY and YL investigated the related references. YL, ZY, ZX and CY performed experiments and wrote the methods. CY and CT analyzed the results. ZX wrote the original draft. CT. YL and ZY confirmed the authenticity of all the raw data. All authors read and approved the final manuscript.

Ethics approval and consent to participate

The present study was conducted with the approval from the Animal Management Committee of the Army Medical University (approval no. SYXK2017002).

Patient consent for publication

Not applicable.

Competing interests

The authors declare that they have no competing interests.

References

1. American Diabetes Association: Diagnosis and classification of diabetes mellitus. Diabetes Care 36 (Suppl 1): S67-S74, 2013.
2. Zhang C, Zhang K, Huang F, Feng W, Chen J, Zhang H, Wang J, Luo P and Huang H: Exosomes, the message transporters in vascular calcification. J Cell Mol Med 22: 4024-4033, 2018.
3. Neuenschwander M, Ballon A, Weber KS, Norat T, Aune D, Schwingshackl L and Schlesinger S: Role of diet in type 2 diabetes incidence: Umbrella review of meta-analyses of prospective observational studies. BMJ 366: l2368, 2019.
4. Li XY, Li QM, Fang Q, Zha XQ, Pan LH and Luo JP: Laminaria japonica polysaccharide inhibits vascular calcification via preventing osteoblastic differentiation of vascular smooth muscle cells. J Agric Food Chem 66: 1821-1827, 2018.
5. Zhan JK, Wang YJ, Wang Y, Tang ZY, Tan P, Huang W and Liu YS: The protective effect of GLP-1 analogue in arterial calcification through attenuating osteoblastic differentiation of human VSMCs. Int J Cardiol 189: 188-193, 2015.

6. Pedersen BK: Anti-inflammatory effects of exercise: Role in diabetes and cardiovascular disease. Eur J Clin Invest 47: 600-611, 2017.
7. Nagano A, Arioka M, Takahashi-Yanaga F, Matsuzaki E and Sasaguri T: Celecoxib inhibits osteoblast maturation by suppressing the expression of Wnt target genes. J Pharmacol Sci 133: 18-24, 2017.
8. Clevers H and Nusse R: Wnt/β-catenin signaling and disease. Cell 149: 1192-1205, 2012.
9. Ravi R, Noonan KA, Pham V, Bedi R, Zhavoronkov A, Ozerov IV, Makarev E, V Artemov A, Wysocki PT, Mehra R, et al: Bifunctional immune checkpoint-targeted antibody-ligand traps that simultaneously disable TGFβ enhance the efficacy of cancer immunotherapy. Nat Commun 9: 741, 2018.
10. Bierie B and Moses HL: Transforming growth factor beta (TGF-beta) and inflammation in cancer. Cytokine Growth Factor Rev 21: 49-59, 2010.
11. Atianand MK, Hu W, Satpathy AT, Shen Y, Ricci EP, Alvarez-Dominguez JR, Bhatta A, Schattgen SA, McGowan JD, Blin J, et al: A long noncoding RNA lincRNA-EPS acts as a transcriptional brake to restrain inflammation. Cell 165: 1672-1685, 2016.
12. Ke Z, Lu J, Zhu J, Yang Z, Jin Z and Yuan L: Down-regulation of lincRNA-EPS regulates apoptosis and autophagy in BCG-infected RAW264.7 macrophages via JNK/MAPK signaling pathway. Infect Genet Evol 77: 104077, 2020.
13. Heydemann A: An overview of murine high fat diet as a model for type 2 diabetes mellitus. J Diabetes Res 2016: 2902351, 2016.
14. Azushima K, Gurley SB and Coffman TM: Modelling diabetic nephropathy in mice. Nat Rev Nephrol 14: 48-56, 2018.
15. Schwarz H, Zhang Y, Zhan C, Malm M, Field R, Turner R, Sellick C, Varley P, Rockberg J and Chotteau V: Small-scale bioreactor supports high density HEK293 cell perfusion culture for the production of recombinant Erythropoietin. J Biotechnol 309: 44-52, 2020.
16. Sun X, Li W, Zhang X, Qi M, Zhang Z, Zhang XE and Cui Z: In vivo targeting and imaging of atherosclerosis using multifunctional virus-like particles of simian virus 40. Nano Lett 16: 6164-6171, 2016.
17. Grieger JC, Soltys SM and Samulski RJ: Production of recombinant adeno-associated virus vectors using suspension HEK293 cells and continuous harvest of vector from the culture media for GMP FIX and FLT1 clinical vector. Mol Ther 24: 287-297, 2016.
18. Chandler RJ, LaFave MC, Varshney GK, Trivedi NS, Carrillo-Carrasco N, Senac JS, Wu W, Hoffmann V, Elkahloun AG, Burgess SM and Venditti CP: Vector design influences hepatic genotoxicity after adeno-associated virus gene therapy. J Clin Invest 125: 870-880, 2015.
19. Wei J, Ran G, Wang X, Jiang N, Liang J, Lin X, Ling C and Zhao B: Gene manipulation in liver ductal organoids by optimized recombinant adeno-associated virus vectors. J Biol Chem 294: 14096-14104, 2019.
20. Li Y, Wan S, Liu G, Cai W, Huo D, Li G, Yang M, Wang Y, Guan G, Ding N, et al: Netrin-1 promotes inflammation resolution to achieve endothelialization of small-diameter tissue engineering blood vessels by improving endothelial progenitor cells function in situ. Adv Sci (Weinh) 4: 1700278, 2017.
21. Jiao L, Zhuang Y, Jiang M, Zhou JH, Wu M, Chen ZJ, Fang JH and Deng YS: Angiopoietin-like 2 has auxo-action in atherosclerosis by promoting atherosclerotic calcification. Int J Clin Exp Pathol 10: 9084-9091, 2017.
22. Fang M, Wang CG, Zheng C, Luo J, Hou S, Liu K and Li X: Mir-29b promotes human aortic valve interstitial cell calcification via inhibiting TGF-β3 through activation of wnt3/β-catenin/Smad3 signaling. J Cell Biochem 119: 5175-5185, 2018.
23. Zhang B, Li Q, Jia S, Li F, Li Q and Li J: LincRNA-EPS in biomimetic vesicles targeting cerebral infarction promotes inflammatory resolution and neurogenesis. J Transl Med 18: 110, 2020.
24. Zou Y, Zhang Y, Church J and Liu X: Comparison of β-catenin and LEF1 immunohistochemical stains in desmoid-type fibromatosis and its selected mimickers, with unexpected finding of LEF1 positivity in scars. Appl Immunohistochem Mol Morphol 26: 648-653, 2018.
25. Wang Q, Wang G, Wang B and Yang H: Activation of TGR5 promotes osteoblastic cell differentiation and mineralization. Biomed Pharmacother 108: 1797-1803, 2018.
26. He J, Zhang N, Zhang J, Jiang B and Wu F: Migration critically meditates osteoblastic differentiation of bone mesenchymal stem cells through activating canonical Wnt signal pathway. Colloids Surf B Biointerfaces 171: 205-213, 2018.
27. Shioi A and Ikari Y: Plaque calcification during atherosclerosis progression and regression. J Atheroscler Thromb 25: 294-303, 2018.
28. Chiarella E, Aloisio A, Scicchitano S, Lucchino V, Montalcini Y, Galasso O, Greco M, Gasparini G, Mesuraca M, Bond HM and Morrone G: ZNF521 represses osteoblastic differentiation in human adipose-derived stem cells. Int J Mol Sci 19: 4095, 2018.
29. Liu Y, Lin F, Fu Y, Chen W, Liu W, Chi J, Zhang X and Yin X: Cortistatin inhibits calcification of vascular smooth muscle cells by depressing osteoblastic differentiation and endoplasmic reticulum stress. Amino Acids 48: 2671-2681, 2016.
30. Rong S, Zhao X, Jin X, Zhang Z, Chen L, Zhu Y and Yuan W: Vascular calcification in chronic kidney disease is induced by bone morphogenetic protein-2 via a mechanism involving the Wnt/β-catenin pathway. Cell Physiol Biochem 34: 2049-2060, 2014.
31. Nagashima M, Sakai A, Uchida S, Tanaka S, Tanaka M and Nakamura T: Bisphosphonate (YM529) delays the repair of cortical bone defect after drill-hole injury by reducing terminal differentiation of osteoblasts in the mouse femur. Bone 36: 502-511, 2005.
32. Rudijanto A: The role of vascular smooth muscle cells on the pathogenesis of atherosclerosis. Acta Med Indones 39: 86-93, 2007.
33. Guzik TJ, Korbut R and Adamek-Guzik T: Nitric oxide and superoxide in inflammation and immune regulation. J Physiol Pharmacol 54: 469-487, 2003.
34. Beck PL, Xavier R, Wong J, Ezedi I, Mashimo H, Mizoguchi A, Mizoguchi E, Bhan AK and Podolsky DK: Paradoxical roles of different nitric oxide synthase isoforms in colonic injury. Am J Physiol Gastrointest Liver Physiol 286: G137-G147, 2004.
35. Niedbala W, Besnard AG, Nascimento DC, Donate PB, Sonego F, Yip E, Guabiraba R, Chang HD, Fukada SY, Salmond RJ, et al: Nitric oxide enhances Th9 cell differentiation and airway inflammation. Nat Commun 5: 4575, 2014.
36. de Seigneux S and Martin PY: Phosphate and FGF23 in the renoprotective benefit of RAAS inhibition. Pharmacol Res 106: 87-91, 2016.
37. Jüppner H: Phosphate and FGF-23. Kidney Int Suppl 79: S24-S27, 2011.